



ORIGINAL ARTICLE

Design of plasticized proton conducting Chitosan: Dextran based biopolymer blend electrolytes for EDLC application: Structural, impedance and electrochemical studies



Jihad M. Hadi^a, Shujahadeen B. Aziz^{b,c,*}, M.F.Z. Kadir^d, Yaser A. El-Badry^e, Tansir Ahamad^f, Enas E. Hussein^g, Ahmad S.F.M. Asnawi^h, Ranjdar M. Abdullah^b, Saad M. Alshehri^f

^a Department of Medical Laboratory of Science, College of Health Sciences, University of Human Development, Kurdistan Regional Government, Iraq

^b Hameed Majid Advanced Polymeric Materials Research Lab., Physics Department, College of Science, University of Sulaimani, Qlyasan Street, Sulaimani 46001, Kurdistan Regional Government, Iraq

^c Department of Civil Engineering, College of Engineering, Komar University of Science and Technology, Sulaimani 46001, Kurdistan Regional Government, Iraq

^d Centre for Foundation Studies in Science, University of Malaya, Kuala Lumpur 50603, Malaysia

^e Chemistry Dept., Faculty of Science, Taif University, Khurma, P.O. Box 11099, Taif 21944, Saudi Arabia

^f Department of Chemistry, King Saud University, P.O. Box 2455, Riyadh 11451, Saudi Arabia

^g National Center of Water Research, Cairo, Egypt

^h Chemical Engineering Section, Universiti Kuala Lumpur Malaysian Institute of Chemical & Bioengineering Technology (UniKL MICET), 78000 Alor Gajah, Malacca, Malaysia

Received 21 June 2021; accepted 17 August 2021

Available online 1 September 2021

KEYWORDS

Biopolymer;
Blending;
FTIR;
Impedance;

Abstract In this work, for the use of an electrical double-layer capacitor (EDLC) device applications, the fabrication and characterization of solid polymer electrolytes (SPEs) based on chitosan-dextran (CS-DN) blended polymer doped and plasticized with ammonium thiocyanate (NH_4SCN) and glycerol are studied, respectively. The Fourier transform infrared (FTIR) spectroscopy method has been used to investigate the structural behavior of electrolytes. It was observed that the FTIR

* Corresponding author at: Hameed Majid Advanced Polymeric Materials Research Lab., Physics Department, College of Science, University of Sulaimani, Qlyasan Street, Sulaimani 46001, Kurdistan Regional Government, Iraq.

E-mail address: shujahadeenaziz@gmail.com (S.B. Aziz).

Peer review under responsibility of King Saud University.



bands are shifted and decreased in their intensities with the increased glycerol plasticizer content and it results in the complex formation. According to the electrical impedance spectra (EIS), the electrolyte incorporated with high contents of plasticizer (42 wt%) revealed the highest ionic conductivity of $(3.08 \times 10^{-4} \text{ S/cm})$. The electrical equivalent circuits (EEC) were used to investigate the circuit elements of the electrolytes further. Increasing glycerol plasticizers verified an improvement in ions density number (n), mobility (μ), and diffusion coefficient (D). The transference number measurements (TNM) indicated that the predominant charge carriers in the conduction process are ions where the (t_{ion}) is 0.95. According to the linear sweep voltammetry (LSV) study, the uppermost conducting sample was found to have sufficient anode stability with a breakdown voltage of 1.9 V that can be used in electrochemical devices. The absence of peaks in the cyclic voltammetry (CV) demonstrated that the charge storage mechanism within the constructed EDLC is fully capacitive. Based on this finding, the starting specific capacitance (C_s), energy density (E_d), and power density (P_d) have been identified to be 118F/g, 13.2 Wh/kg, and 1560 W/kg, respectively. Throughout its 100 cycles, the equivalence series resistance ESR value was between 53 and 117 Ω .

© 2021 The Author(s). Published by Elsevier B.V. on behalf of King Saud University. This is an open access article under the CC BY-NC-ND license (<http://creativecommons.org/licenses/by-nc-nd/4.0/>).

1. Introduction

Energy storage devices are almost found everywhere in high energy consumption communities, for instance, powering our mobile devices and computers. Polymer electrolyte (PE) is used commonly in advanced chemical energy storage technology, such as supercapacitor, solar cells, protonic and fuel cells. Therefore, solid polymer electrolyte (SPE) film has gotten much attention because it has many advantages over other types of electrolytes (Luo et al., 2015; Hadi et al., 2020; Hamsan et al., 2020). Natural ingredients and biomaterials are strong candidates for research activities due to increases in the consciousness of a universal crisis. Over decades, researchers have used biopolymers as the polymer host for electrolytes because of their outstanding properties, for instance, their compatibility with a broad variety of solvents and salts and ease of film-forming (Hamsan et al., 2019; Chai and Isa, 2016). Also, they are obtained sustainably from a wide variety of natural resources. Besides all else, the environmentally safe characteristics of the biopolymeric materials will assist to the decrease harm to human healthiness and the environment (Nirmala Devi et al., 2017). The biopolymers will solve the dopant once the lone pair electron of their heteroatoms like nitrogen and oxygen interacts directly with cations from the dopant. Thus, natural polymers as solid biopolymer electrolytes are crucial to be produced (Zhu et al., 2015). Dextran (DN) is a natural polymer produced by the bacteria of *Leocostoc mesenteroides* during reproduction. It has a linear backbone structure with 1,6- α -d-glucopyranoside primary linkage. The inclusion of the two key functional groups (i.e., hydroxyl and glycosidic bond) in its chain structure ensure the ability to use as an ionic conductor (Dumitraşcu et al., 2012; Hamsan et al., 2020). On the other hand, chitosan (CS) comprises of β -(1,4-linkage) of 2-amino-2-deoxy-d-glucopyranose obtained by N-deacetylation of chitin. Both CS and chitin are found in cramp and shrimp shells. The deacetylation mechanism removes the acetyl groups from the chitin molecular chain, leaving an amino group. Similar to dextran, (CS) structure possesses various oxygen-containing functional groups (Hadi et al., 2020; Du et al., 2017; Mobarak et al., 2013).

In combination with avoiding environmental pollution, which is caused by the use of lithium salts, numerous studies have shown that the ammonium salts possess favorable polymer electrolyte properties with relatively high dissociation of ions such as NH_4SCN (Selvalakshmi et al., 2017), NH_4Br (Shukur et al., 2019), NH_4NO_3 (Aziz et al., 2021), NH_4I (Mustafa et al., 2020), and NH_4F (Ramlli and Isa, 2016). In addition to that, high ionic conductivity could be obtained by including NH_4^+ and H^+ using ammonium-based salts.

Also, the NH_4SCN has a low lattice energy of (572 KJ/mol) thus, the electrolyte requires less energy to destroy the ionic bonds (Shamsuri et al., 2020).

The most crucial objective in the polymer electrolyte is to optimize ionic conductivity. One of the promising techniques for improving ionic conductivity is plasticization. This process incorporates a combination between the polymer and a low molecular weight plasticizer, which helps dissolve and dissociate salts and making more facilities to the charge carrier mobilities (Nasef et al., 2007). Many polymer electrolytes used in an energy storage device are formulated with glycerol to improve ionic conductivity and other significant parameters. Moreover, glycerol is identifying to enhance the ionic conductivity up to 10^{-3} S/cm via increasing more channels for ion conduction, suggesting a satisfactory outcome in device application (Rani et al., 2015).

Supercapacitors (SCs) are classified into three types: electrical double-layer capacitors (EDLCs), pseudocapacitors (PCs), and hybrid capacitors (HCs) (Iro et al., 2016). Conducting polymer and metal oxide electrodes have been used in pseudocapacitors (PCs), and energy is stored using a Faradaic method. Unlike (PCs), (EDLC) undergoes a non-Faradaic reaction in which a double layer of charges forms on the surface of the carbon electrodes. On the other hand, the (PCs) and (EDLC) mechanisms are combining in hybrid capacitors (HCs) (Shobana et al., 2015; Nofal et al., 2020; Kiamahalleh et al., 2012). Meanwhile, the (EDLCs) are distinct from the other two capacitors by high power density, less weight, durability, and ease of fabrication. The use of activated carbon (ACs) to obtain good compatibility with polymer electrolytes has been extensively studied. The benefits of the (ACs) for the (EDLC) applications include cost-effectiveness, high electrical conductivity, excellent chemical stability, and a broad superficial area (Aziz et al., 2020). Due to the need for high conducting SPE for the EDLC device, this work attempts to fabricate high conducting CS-Dextran- NH_4SCN -Glycerol based solid polymer electrolyte.

2. Experimental details

2.1. Raw materials

The host polymeric materials utilized in this study are chitosan (CS) and dextran with the average molecular weights of (310,000–375,000 g/mole) and (35,000–45,000 g/mole), respectively. Ammonium thiocyanate NH_4SCN (76.12 g/mole), and low molecular weight of glycerol ($\text{C}_3\text{H}_8\text{O}_3$) (92 g/mole), acetic acid (CH_3COOH) (60 g/mole). Sigma-Aldrich (Kuala Lumpur,

Malaysia) provided all the above chemicals and directly used them without purification. Furthermore, activated carbon (AB), carbon black (CB) with the molecular weights of (12 g/mole), and polyvinylidene fluoride (PVdF) (534,000 g/mole) were acquired from Magma value.

2.2. Electrolyte preparation

To fabricate the CS-Dextran-based polymer blending, 60 wt% of chitosan with 40 wt% dextran has dissolved individually at ambient temperature in 50 mL acetic acid (1%) solution for ~90 min. Afterward, these individual solutions were then blended and stirred continuously for ~3 h to achieve a homogeneous blending solution. Then, a constant quantity of NH_4SCN (40 wt%) was then dissolved in the solution with continuous stirring using a magnetic stirrer to attain a polymer electrolyte based on CS-Dextran- NH_4SCN . Subsequently, CS-Dextran-40 % NH_4SCN was glycerolized using different quantities of glycerol from 14 to 42 wt% in stages of 14. The prepared electrolytes were labeled as CSDXG1, CSDXG2, and CSDXG3 for the CS-Dextran- NH_4SCN incorporated with 14, 28, and 42 wt% of glycerol, respectively. The solution's ingredients were stirred and then poured into plastic Petri dishes left untouched at ambient temperature to produce a homogenous solution. The electrolytes were stored in a blue Silica gel desiccator for future drying before the EDLC characterization.

2.3. FTIR and EIS characterization

The FTIR spectra in the range of 650–3850 cm^{-1} with a resolution of 1 cm^{-1} were acquired using a Spotlight 400 spectrometer (Perkin Elmer, Waltham, MA, USA) to validate the polymer blend electrolyte formation. Electrochemical impedance spectroscopy (EIS) was utilized to investigate the electrochemical characteristics of the materials, with spectra attained using a 3532–50 LCR HiTESTER (Hioki, Nagano, Japan) in the frequency range of 50 Hz–5,000,000 Hz. The electrolyte's thickness was fixed from 150 to 152 μm and located between a pair of stainless-steel (SS) electrodes. The cell was linked to a computer and fitted with software to measure the real (Re-Z) and imaginary (Im-Z) fragments of complex impedance spectroscopy (Com-Z).

2.4. Transference number measurement (TNM) study

The ion (t_{ion}) and electron (t_{el}) transport numbers have been determined by keeping a voltage of 0.2 V while polarizing a cell of SS/highest conducting sample/SS. The ion transference number was estimated at ambient temperature using a DP 3003 digital DC power supply (V & A instrument, Shanghai, China).

2.5. Linear sweep voltammetry (LSV) study

LSV was used to determine the maximum operating voltage of the most conducting CS-Dextran- NH_4SCN -glycerol system via a Digi-IVY DY2300 potentiostat. The LSV was measured in the potential range of between 0 and 2.5 V at a sweep rate of 10 mV/s. The cell arrangement was identical to that seen in the TNM.

2.6. EDLC fabrication

The solvent and carbonaceous materials are commonly used in the preparation of the EDLC electrodes. There were made with 0.25 gm of carbon black (CB), 3.25 gm of activated carbon (AC), and 0.5 gm of polyvinylidene fluoride (PVdF). The dry mixing of carbonaceous materials was done with a planetary ball miller (XQM-0.4) at 500 rounds/minutes for ~18 min. Next, all of the powders mentioned above were dissolved and constantly stirred in 20 mL of N-methyl pyrrolidone (NMP) solvent until a dark black solution has obtained. A solution is then coated with aluminum foil using a doctor blade method. Afterward, a coated aluminum foil was dried in an oven for a certain period at ~60 °C. A Silica gel desiccator was used to remove the excess moisture from the electrodes. The comparatively highest conducting sample was placed between two activated carbon electrodes and packed in CR2032 coin cells. Finally, the Digi-IVY DY2300 potentiostat was used at different scan rates of 10, 20, 50, and 100 mV/s ranging from 0 to 0.9 V to perform cyclic voltammetry (CV) of the constructed EDLC.

3. Result and discussion

3.1. FTIR study

The FTIR technique has been performed to examine the interactions between atoms and ions of the CS-Dextran- NH_4SCN glycerol-based electrolyte. Variations in the vibrational modes in the polymer electrolyte may also result from such interactions. Fig. 1 depicts the FTIR spectra of an SPE based on the CS-Dextran- NH_4SCN -glycerol at a wavenumber ranging from 650 to 3850 cm^{-1} (Shukur et al., 2016; Aziz et al., 2021; Nofal et al., 2021). A broad peak at ~3300 cm^{-1} is due to O-H stretching modes. There was a shift and turn down in its intensity in the glycerolized CS-Dextran- NH_4SCN , resulting in an interaction between electrolyte components (Brza et al., 2021). The considerable chain flexibility in dextran around the glycosidic linkage corresponds to the appearance of a peak at 1020 cm^{-1} . Also, dextran is responsible for appearing a C-H stretching peak at ~2900 cm^{-1} since such a band is not existing in the FTIR spectra of CS (Vettori et al., 2012). A sharp peak is observable at ~2000 cm^{-1} , attributing to aromatic stretching of the NH_4SCN salt. Therefore, its intensity shifts and lowers with the increment of glycerol plasticizer through the interactions of blend polymers with the electrolyte components (Hemalatha et al., 2019). The peak perceived at ~1000 cm^{-1} indicates that there is substantial chain flexibility of the dextran backbone. The C-H bending typically emerged around ~1430 cm^{-1} , while a band begins ~1150 cm^{-1} , showing asymmetrical C-O-C ring stretching. The occurrence of C-O bands is responsible for the strong peak at ~1008 cm^{-1} and the tiny one at ~1095 cm^{-1} . Two peaks that emerged at ~1540 cm^{-1} and ~1610 cm^{-1} were associated with amide bonds (NH_2) and carboxamide ($\text{O}=\text{C}-\text{NH}-\text{R}$). Changes in amide bonds (NH_2) and carboxamide ($\text{O}=\text{C}-\text{NH}-\text{R}$) suggest a complexation between CS:Dextran blend polymers with electrolyte components. As a way of achieving the greater molecular mass resulting from cation binding, this cation salt to oxygen and

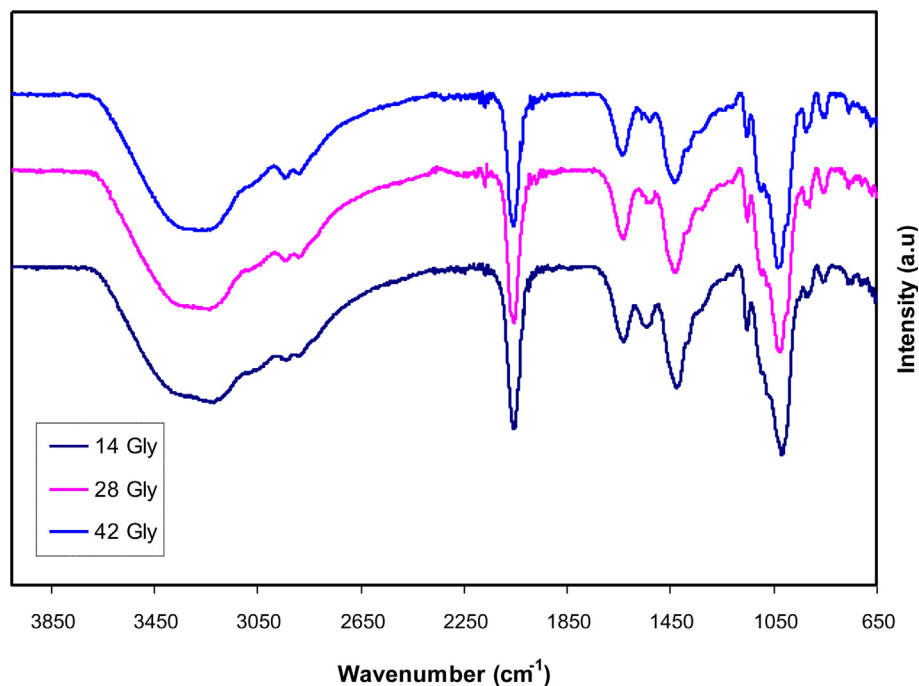


Fig. 1 Fourier transform infrared (FTIR) spectra for glycerolized the CS-Dextran-NH₄SCN at a wavenumber ranging from 650 to 3850 cm⁻¹.

nitrogen atom attachments lessens the vibrational intensity of the (NH₂) and (O=C—NH—R) bonds, resulting in both lowering and shifting in peak intensities (Dumitraşcu et al., 2011; Wei et al., 2009; B. Aziz et al., 2020). A fascinating observation is that the inclusion of glycerol into the CS-Dextran-NH₄SCN polymer-salt complexation results in a dramatic shift in their band intensity. The incorporation of glycerol leads to dissociate more salts to anions and cations, which means that more ions are produced to interact with CS-Dextran. It is noteworthy that variations in the strength of these bands have been strongly related to changes in macromolecular order (Liang et al., 2009).

The FTIR spectra of the electrolytes show a broad peak at the region between 2015 and 2090 cm⁻¹ which is related to the SCN⁻ stretching mode. Based on the literature (Zhang et al., 2003; Ramya et al., 2007), this broad envelope results from the overlap of three narrower peaks. These peaks are located at ~2040 cm⁻¹, ~2055 cm⁻¹, and ~2070 cm⁻¹ showing the free anion (SCN⁻), contact ion pair (NH₄⁺, SCN⁻), and ion aggregate, respectively. Thus, the deconvolution method is used to separate the peaks using Origin Pro software. In the 2015 and 2090 cm⁻¹ regions, the transmittance spectra were converted to absorbance spectra. Then baseline correction was performed for each FTIR spectrum. Fig. 2 (a-c) shows the FTIR deconvolution spectra of SCN⁻ stretching modes in CS:Dex:NH₄SCN:glycerol.

At 14 wt% glycerol, free ion, contact ion pair, and ion aggregate have 18.43%, 55.85%, and 25.71%, respectively. By increasing the glycerol at 28 wt% and 42 wt%, the percentage of free ions increased to 23.84% and 27.85%, respectively. The percentage area of the contact ion pair is decreased with increasing glycerol. The percentages of ion carriers are shown in Table 1. Noor and Isa (2019) reported the same result for the CMC-NH₄SCN electrolyte system. Woo et al. (2011) used

the FTIR deconvolution method for the SCN⁻ stretching mode in the poly(ε-caprolactone) (PCL)-NH₄SCN electrolyte system to show the aggregation of ions. Their result showed that the number of free ions was maximum at 26 wt% NH₄-SCN salt (Woo et al., 2011).

The free ion percentage, contact ion pair, and ion aggregate were measured by the area under each band of FTIR and calculated by the below equations (Noor and Isa, 2019).

$$\text{Percentage of free ions (\%)} = \frac{A_f}{A_f + A_c + A_a} \times 100\% \quad (1)$$

$$\begin{aligned} \text{Percentage of contact ion pairs (\%)} \\ = \frac{A_c}{A_f + A_c + A_a} \times 100\% \end{aligned} \quad (2)$$

$$\begin{aligned} \text{Percentage of ion aggregates (\%)} \\ = \frac{A_a}{A_f + A_c + A_a} \times 100\% \end{aligned} \quad (3)$$

where A_f is the area under the peak of the free ion's region, A_c is the area under the peak of the contact ion pair region, and A_a is the area under the peak of the ion aggregate region.

3.2. Impedance study

Electrochemical impedance spectroscopy (EIS) is a powerful and reliable method for investigating various electrical characteristics of electrolyte materials (Polu and Kumar, 2011). The plots of the CS-Dextran-NH₄SCN containing 14, 28, and 42 wt% of glycerol concentrations using impedance spectroscopy (Re-Z vs. Im-Z) were presented in Fig. 3(a-c), respectively. The responses of the EIS are often distinguished by a half circle and a tail in high and low-frequency regions. In this

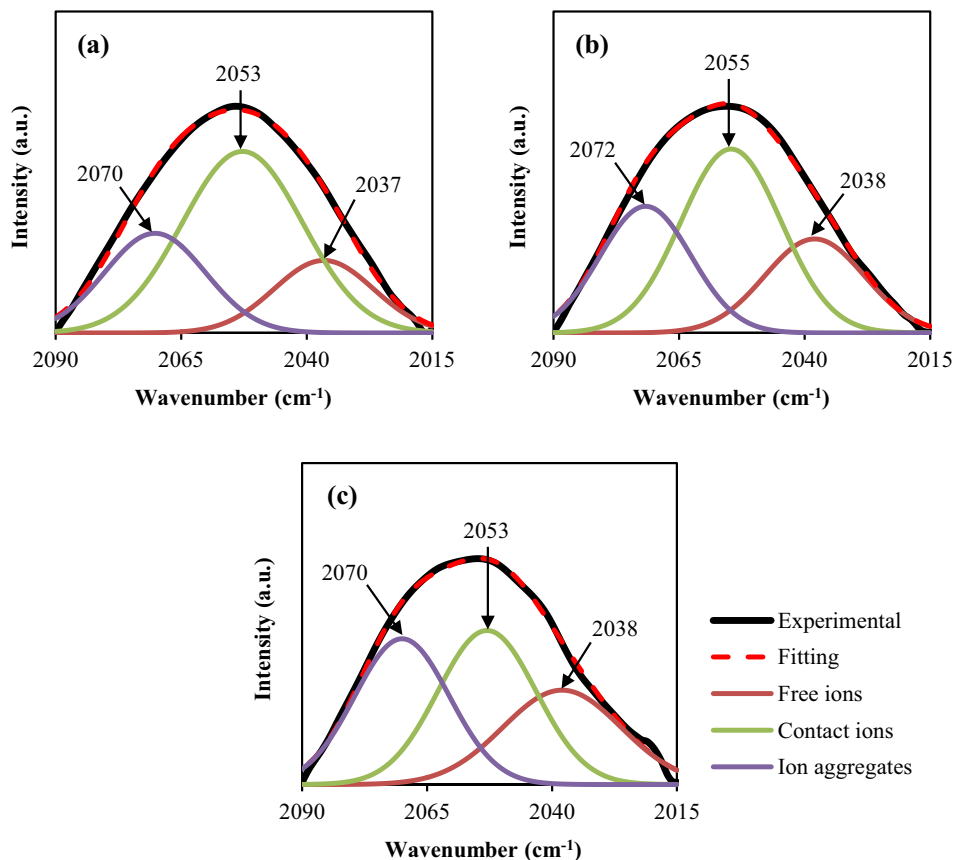


Fig. 2 Deconvolution (DVN) of the FTIR spectra at a wavenumber between 2015 and 2090 cm^{-1} .

study, there is no semicircle has appeared, indicated that there is no electron reaction at the electrode–electrolyte interfaces. Meanwhile, it is also representing the migration of ions from the electrolyte to the surface of the electrodes to produce the double-layer capacitance (Hadi et al., 2020). The Nyquist plots display the removal of the high-frequency semicircle portion, leading to the conclusion that the overall conductivity is mainly ion conduction.

On the other hand, the spike appearance at low frequencies is due to forming an electric double-layer at the blocking electrodes. EIS measurements in this investigation are displaying a similar behavior to the previous studies, as shown in Fig. 3(a-c) (Aziz et al., 2021). Consequently, the effect of electrode polarization (EP) is induced by the creation of an electric double layer, resulting in ions accumulated at the electrode–electrolyte interfaces. Therefore, ions cannot traverse the system due to the electrical behavior of stainless-steel (SS) electrodes, and hence the imaginary (Im-Z) and the real (Re-Z) parts of impe-

dance spectroscopy could be measured in different frequencies, resulting in impedance plots.

The electrical equivalent circuit (EEC) technique has been utilized to analyze the EIS because it is uncomplicated and gives the whole image of the system. In the electrolyte system, EEC comprises a pair of constant phase elements (CPEs) which are (CPE1) and (CPE2) with including bulk resistance R_b for the ion carriers (see Fig. 3). Both R_b and (CPE) are connected in parallel at high-frequency areas and in series with (CPE2) at low-frequency areas where a double-layer capacitance is generated. The impedance of CPE (Z_{CPE}) is calculated using Eq. (4):

$$Z_{CPE} = \frac{1}{C\omega^p} \left[\cos\left(\frac{\pi p}{2}\right) - i \sin\left(\frac{\pi p}{2}\right) \right] \quad (4)$$

where CPE capacitance, plot's deviation measure from the axis, and angular frequency are denoted by C , P , and ω . Also, the impedance values of (Re-Z) and (Im-Z) could be mathematically expressed as follows:

$$Z_r = R + \frac{\cos(\pi n/2)}{C\omega^n} \quad (5)$$

$$Z_i = \frac{\sin(\pi n/2)}{C\omega^n} \quad (6)$$

Here, n is associated to the imaginary axis deviation of the Nyquist plot. It is demonstrated that the Nyquist plot reveals that the electrolyte's resistive component is dominant. The polymers may also act as an insulator, and the CPE and R_b

Table 1 The values of transport parameters of glycerolized the CS-Dextran- NH_4SCN systems.

Glycerol (wt.%)	14%	28%	42%
Free ion	18.43%	23.84%	27.85%
Ion's aggregate	25.71%	29.36%	34.44%
Contact ion	55.85%	46.80%	37.71%

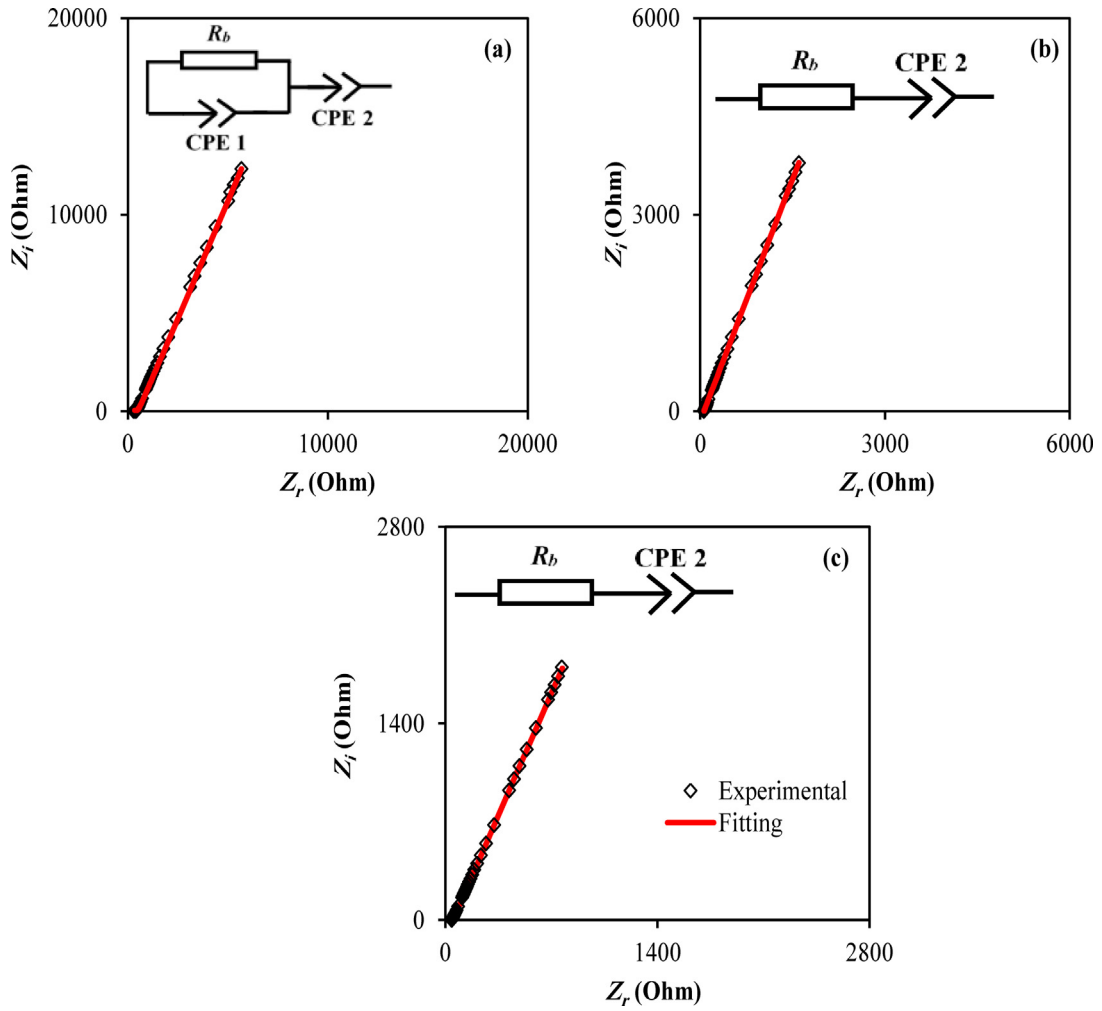


Fig. 3 Complex plots of impedance spectra for the CS-Dextran-NH₄SCN systems containing various amounts of glycerol.

are linked together in series as demonstrated in Fig. 3(a-c) inset. Table 2 summarizes the EEC's parameters fitting for the CS-Dextran-NH₄SCN systems containing various amounts of glycerol (wt.%) (Hadi et al., 2020).

In order to evaluate the (σ_{dc}) ionic conductivity of the CS-Dextran-NH₄SCN containing various amounts of glycerol based on the bulk resistance R_b value, it is essential to use the following equation:

$$\sigma_{dc} = \left(\frac{1}{R_b}\right) \times \left(\frac{l}{A}\right) \quad (7)$$

where A represents the electrolyte area, and l denotes the thickness of the electrolyte (Malathi et al., 2010; Qian et al.,

2001; Aziz et al., 2020). Table 3 summarizes the (σ_{dc}) ionic conductivity of glycerolized CS-Dextran-NH₄SCN systems. From the equation shown above, the relation between the R_b and σ_{dc} is disproportional. It can be observed that increasing the glycerol weight percent from 14 to 42 wt% to the system leads to reduce the bulk resistance value, demonstrating the increment in the ionic conductivity. It is generally recognized and mathematically expressed that the link between ionic conductivity of the electrolytes with ions density and mobility is:

$$\sigma = \sum \eta q \mu \quad (8)$$

where the charge carrier density is denoted by η and q represents the simple charge, μ stands for the ionic mobility. The

Table 2 The EEC's parameters fitting for the generated system.

Glycerol (wt.%)	P1	P2	K1	K2	CPE1	CPE2
14 Gly	0.27	0.75	9.00×10^4	8.65×10^5	1.11×10^{-5}	1.16×10^{-6}
28 Gly	0.38		2.75×10^5	–	3.64×10^{-6}	–
42 Gly	0.37		1.31×10^5	–	7.63×10^{-6}	–

Table 3 Shows ionic conductivity (σ_{dc}) for CS-Dextran-NH₄-SCN systems, containing various amounts of glycerol at room temperature.

Glycerol (wt.%)	Ionic conductivity σ_{dc} (S. cm ⁻¹)
14	2.80×10^{-5}
28	2.57×10^{-4}
42	3.08×10^{-4}

σ_{dc} of the polymer electrolyte applicable in energy storage devices like EDLC and batteries must range from 10^{-3} to 10^{-5} S/cm (Aziz et al., 2021; Awasthi and Das, 2019). The highest ionic conductivity obtained in this work is 3.08×10^{-4} S/cm for the electrolyte incorporated with 42 wt % of glycerol. Aziz et al. (B. Aziz et al., 2020) have reported a comparable value in the (σ_{dc}) for glycerolized the CS-Dextran-NH₄PF₆.

The transport parameters of the number of density (n), diffusion coefficient (D), and ions mobility (μ) are estimated through the following equations using impedance data. The ion diffusion is computed from Eqs. (9) and (10):

$$D = D_0 \exp\{-0.0297[\ln D_0]^2 - 1.4348 \ln D_0 - 14.504\} \quad (9)$$

$$D_0 = \left(\frac{4k^2 l^2}{R_b^4 \omega_{min}^3} \right) \quad (10)$$

where l is the electrolyte's thickness, and ω_{min} stands for the angular frequency at the lowest Z_i value. The ions mobility is calculated using Eq. (11):

$$\mu = \left(\frac{eD}{K_b T} \right) \quad (11)$$

Here K_b represents the Boltzmann constant, and T denotes the absolute temperature.

Eq. (7) provides the (σ_{dc}) ionic conductivity, and thus, the number of ions density is derived using Eq. (8) (Aziz et al., 2021).

The characteristics related to ion transport for all of the systems have provided in Table 4. There is a definite tendency of rising parameters value of (n), (D), and (μ) with increasing glycerol concentration into the CS-Dextran-NH₄SCN systems from 14 to 42 wt%. The enrichment of chain flexibility in the inclusion of glycerol is the cause of these correlations. As a consequence of all of this leads to an increment in conductivity. Glycerol molecules play a crucial role in boosting the dissociation of the NH₄SCN salt, increasing the density of charge

Table 4 The values of n, μ , and D for the CS-Dextran-NH₄-SCN systems, containing various amounts of glycerol at room temperature.

Glycerol (wt.%)	n	μ	D
14	1.24×10^{22}	1.42×10^{-8}	3.69×10^{-10}
28	2.87×10^{22}	5.60×10^{-8}	1.46×10^{-9}
42	3.12×10^{22}	6.17×10^{-8}	1.61×10^{-9}

carriers. Furthermore, the attractive forces between the opposite ions of the salt are considerably reduced. Therefore, NH₄-SCN has generated a high density of NH₄⁺ ions inside the system (Samsudin and Isa, 2012; Brza et al., 2020; Arof et al., 2014). The σ_{dc} ionic conductivity obtained in this work has found to be higher and comparable to other electrolyte systems using various ammonium salts as reported in literature and summarized in Table 5.

3.3. TNM study

It is of immense significance that the transport ions, t_{ion} value of an electrolyte needs to be near an ideal value of unity for use in the applications of the EDLC. The primary charge carrier inside the polymer electrolyte is validated using TNM. Ions rather than electrons are usually the primary charge carriers. In this case, NH₄⁺ and SCN⁻ ions are responsible for the adsorption reaction at the surface of the activated carbon electrodes. The polarization curve of current against time for the highest conducting electrolyte is portrayed in Fig. 4, at the working potential of 0.2 V (Nik Aziz et al., 2010; Rani et al., 2018; Shuhaimi et al., 2012).

Subsequently, the following relations were used to calculate the t_{ion} and t_{el} of glycerolized the CS-Dextran-NH₄SCN sample, as it was located between pair of stainless-steel (SS) electrodes.

$$t_{ion} = \frac{I_i - I_{ss}}{I_i} \quad (12)$$

$$t_{el} = 1 - t_{ion} \quad (13)$$

where t_{ion} and t_{el} denote transport ions and electrons, respectively, I_i denotes the initial current, which includes both electrons and ions, and I_{ss} is the steady-state current that covers electrons only. The initial total current was found to be 4.3 μ A, as can be seen in Fig. 4. Following that, the current starts to drop until it reaches a saturation point. The high value of the initial current is due to both ions and electrons at the initial stage. However, results from the lack of ionic species induce an extreme drop in the current value. In this study, the t_{ion} value was found to be 0.95, close to the ideal value, implying that ions in the (CS-Dextran-NH₄SCN-glycerol) system govern the transport mechanism (Wang et al., 2018; Shanmuga Priya et al., 2018; Samsudin et al., 2014; Polu and Kumar, 2013). Our previous study for the CS-MC- NH₄SCN-glycerol (Aziz et al., 2021) showed the t_{ion} value of 0.976, comparable with this work. The t_{ion} value of 0.86 in the CS-Dextran-NH₄Br system (Aziz et al., 2021) without plasticizer suggests that the glycerol plasticizer enhanced the movement of the ions inside the system.

3.4. LSV study

For fabricating an energy device system, the determining potential stability window (PSW) is fundamental. The linear sweep voltammetry (LSV) technique is an important feature to identify the electrolyte's breakdown voltage. The curve of decomposed voltage for the uppermost conducting sample has shown in Fig. 5 at the working voltage of 10 mV/s (Kadir and Arof, 2011). In the range of 0–1.8 V, there are no visible current fluctuations in the LSV plot. When the potential

Table 5 The ionic conductivity σ_{dc} and the EDLC parameters value using various solid biopolymer electrolytes have reported in other words as a comparison.

SPEs	σ_{dc} (S. cm ⁻¹)	LSV (V)	Cs (F/g)	E _d (Wh/kg)	P _d (W/kg)	Ref.
DN-NH ₄ NO ₃ -Gly	1.15×10^{-3}	1.75	16.1 at 0.5 mV/s	1.62	206	(Hamsan et al., 2020)
DN-NH ₄ NO ₃	3×10^{-5}	–	–	–	–	(Hamsan et al., 2019)
DN-NH ₄ Br	1.67×10^{-6}	1.62	2.46 at 50 mV/s	–	–	(Hamsan et al., 2020)
CS-NH ₄ Br-Gly	1.9×10^{-4}	1.8	7.5 at 10 mV/s	–	–	(Shukur et al., 2019)
CS-DN-NH ₄ I	5.16×10^{-3}	1.8	67.5 at 100 mV/s	7.59	520	(B. Aziz et al., 2020)
CS-DN-NH ₄ PF ₄ -Gly	3.06×10^{-4}	1.5	23.1 at 100 mV/s	11.6	2741	(B. Aziz et al., 2020)
CS-DN-NH ₄ F	1×10^{-3}	1.7	12.4 at 100 mV/s	1.4	428	(Aziz et al., 2019)
CS-DN-NH ₄ SCN	1.28×10^{-4}	–	–	–	–	(Kadir and Hamsan, 2018)
Starch-CS-NH ₄ SCN	1.3×10^{-4}	–	–	–	–	(Mohamed et al., 2020)
DN-PVA-NH ₄ SCN	8.03×10^{-3}	3.01	–	–	–	(Maheshwari et al., 2021)
CS-DN-NH ₄ SCN-Gly	3.08×10^{-4}	1.9	64.24 at 10 mV/s	13.2	15.60	This work

Where NH₄NO₃ is the ammonium nitrate, NH₄Br is the ammonium bromide, Gly stands for glycerol, NH₄I is the ammonium iodide, NH₄PF₄ is the ammonium hexafluoro phosphate, NH₄F is the ammonium fluoride, and PVA is the polyvinyl alcohol.

approaches 1.9 V, the electrolyte reaches its decomposition voltage, as shown by the onset in current value. Furthermore, a rapid increase in current value indicating occurring electrochemical reaction at this point. This value is suitable for energy storage device applications (Asmara et al., 2011; Sampathkumar et al., 2019). Notably, the findings obtained in this study are comparable to previous studies using ammonium salt-based electrolytes. NG and Mohamad (2008) have documented the breakdown potential of 1.8 V for their system of chitosan-NH₄NO₃-ethylene carbonate-based polymer electrolytes. Also, the system of potato starch-chitosan-NH₄NO₃-glycerol possesses the decomposition potential of 1.88 V (Hamsan et al., 2017). Table 5 shows the σ_{dc} and value

of the EDLC parameters using several solid polymer electrolytes based ammonium salts reported in the literature as a comparison with these findings.

3.5. CV study

The type of charge storage that has occurred at the electrode/electrolyte interfaces could be determined using investigations of cyclic voltammetry (CV) of the EDLC. Fig. 6 depicts the CV of the constructed cell at various sweep ratings of 10, 20, 50, and 100 mV/s. The working potential was ranged from 0 to 0.9 V at room temperature. The following relation was used

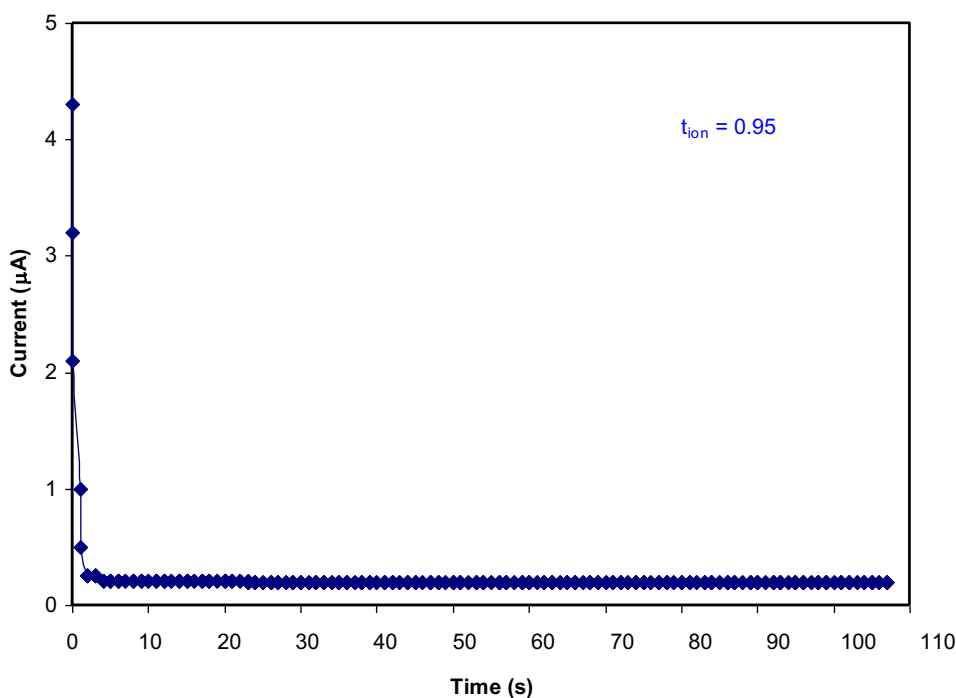


Fig. 4 The polarization curve of current against time for the highest conducting electrolyte.

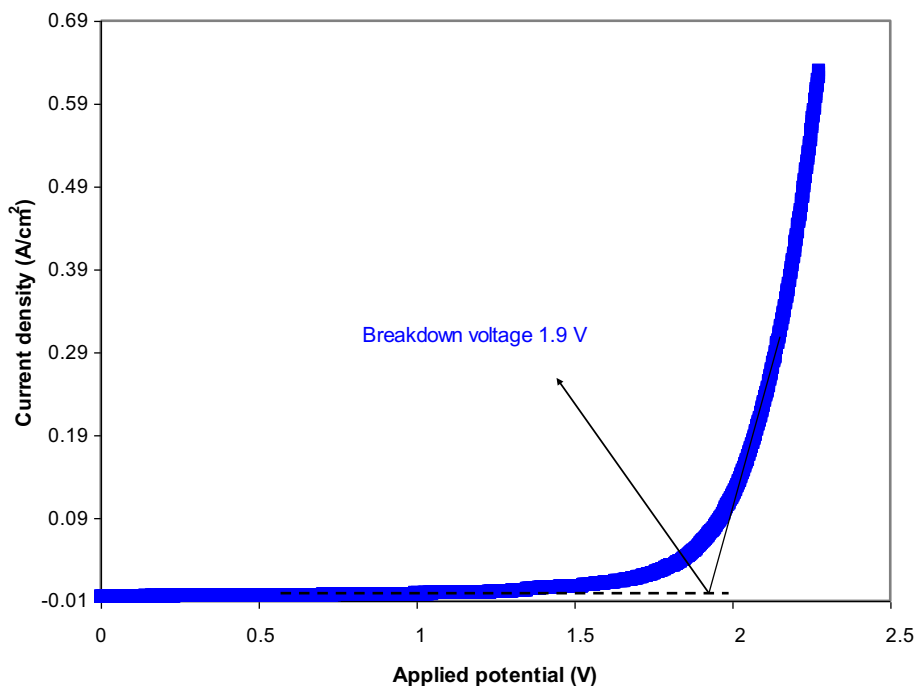


Fig. 5 The LSV plot for the uppermost conducting sample.

to calculate the specific capacitance, C_s , for the fabricated EDLC.

$$C_{cv} = \int_{V_i}^{V_f} \frac{I(V)dV}{2mv(V_f - V_i)} \quad (14)$$

where V_i indicates the starting potential (i.e., 0 V) and V_f stands for the final applied voltage (i.e., 0.9 V) (Hadi et al.,

2020; Chen et al., 2010; Nadiyah et al., 2017). The mass of active material is denoted by m , and v stands for the voltage scan rate (mV/s). The actual area of the CV plot is denoted by $I(V)dV$. Based on the plot, the non-appearance of peaks indicates no reduction/oxidation (redox) reaction in the entire potential range. This phenomenon demonstrates the presence of an electrical double-layer capacitor. The absence of peaks

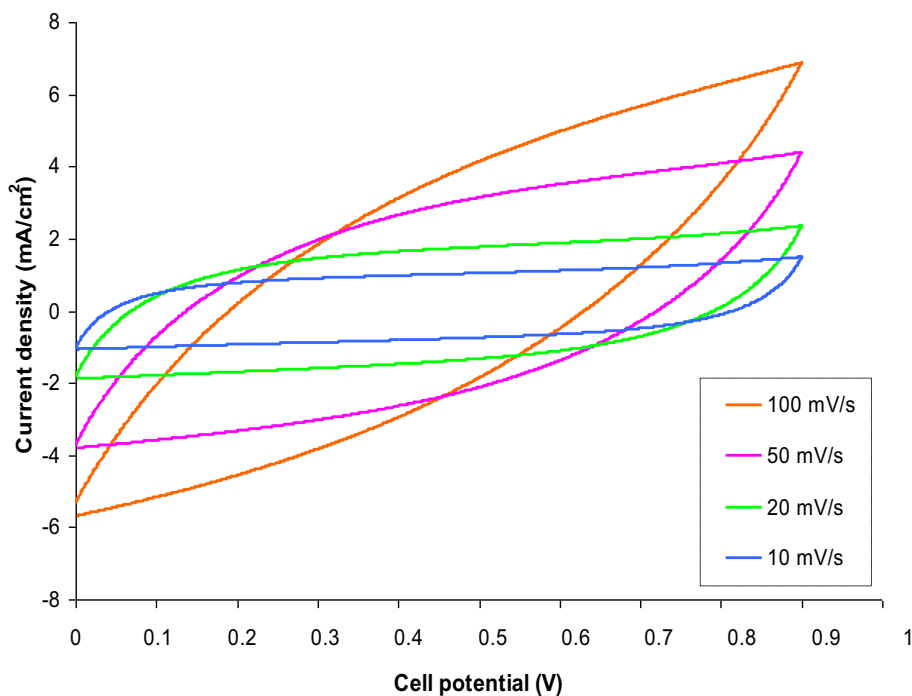


Fig. 6 The CV curve of the constructed cell at various sweep ratings of 10, 20, 50, and 100 mV/s.

reveals that a quick Faradaic reversible reaction has not occurred along with the double-layer formation which supports its EDLC characteristics (Chong Mee Yoke, 2017; Aziz et al., 2019; Wang et al., 2018). The ions accumulation at the interfaces between electrodes and electrolyte once the electrical potential has applied in the EDLC is the basis of the charge-storage process. The capacitance is calculated using Eq. (14). The capacitance at 10, 20, 50, and 100 are found to be 64.24F, 52.01F, 32.14F, and 17.87F, respectively. Thus with increasing scan rates, the capacitance decreased. This is attributed to less charge accumulation at high scan rates. It is noteworthy that the CV profile has a leaf-like form with no discernable peak. However, a slight deviation can be observed from its rectangular shape, attributing to the electrode porosity and also internal resistance. Due to the carbon electrode's porosity, the CV has a relatively high internal resistance, giving it a leaf-like form (Kumar et al., 2012). The obtained specific capacitance C_s of fabricated EDLC is higher compared to some other previous studies (see Table 5).

3.6. Galvanostatic charge–discharge (GCD) characteristics

The EDLC rechargeability has been evaluated through applied a current density of 0.2 mA/cm² and 100 cycles recorded, as demonstrated in Fig. 7. The ions charged in bulk electrolyte begin to migrate into the interface region once current is applied, resulting in a charge double-layer is known as capacitance. A linear discharge curve response verifies the capacitive behavior of the constructed EDLC. Therefore, the voltage drop of discharge characteristics slightly deviates from their triangle-like shape, which could be ascribed to the roughness of the activated carbon, internal resistance, and bulk electrolytes. The linearity of the discharge characteristic also suggests that the charged pore surface and ions have strong pure electrostatic interactions. The GCD curve from their symmetric triangles can be used to detect the presence of the non-Faradaic mechanism. Fig. 8 shows the variation of specific capacitance, C_s for the constructed EDLC up to 100 cycles. The specific capacitance C_s of fabricated EDLC could be measure by the charge–discharge response using the following rela-

tion (Lim et al., 2014; Liew et al., 2016; Aziz et al., 2020; Nadiyah et al., 2015):

$$C_{CD} = \frac{i}{sm} \quad (15)$$

where s stands for the gradient of the discharge region, and i denotes the applied current. The C_s value was determined to be around 118F/g at the 1st cycle, following by a decrease to 100F/g when the cycle reaches its 50th cycle. The inhomogeneity of the electrode/electrolyte area is responsible for the fluctuation in a specific capacitance, C_s value. It is noteworthy that the C_s value is nearly constant over its 100 cycles, verifying its excellent cyclic stability. A slight fluctuation in the C_s -value is attributed to variation in the ionic polarization.

Furthermore, the low lattice energy of the salt should be noted for improving the specific capacitance value, contributing to high dissociation (Aziz et al., 2021; Pandey et al., 2011). The obtained C_s value for the system of CS-Dextran-NH₄F was found to be 12.4F/g, as reported by Aziz et al. (2019). This might be attributed to the lattice energy of the NH₄SCN salt is lower than that of NH₄F. Thereby, the strong interaction between NH₄⁺ with F⁻ is therefore expected compared to NH₄⁺ with SCN⁻.

The drop in voltage (V_d) can be observed at the beginning of the discharging process, as shown in Fig. 7. It is demonstrating the internal resistance of the constructed EDLC called equivalence series resistance (ESR), which was calculated using the following equation:

$$ESR = \frac{V_d}{i} \quad (16)$$

where V_d represents the drop voltage. Fig. 9 displays the ESR value against cycle numbers up to 100 cycles. One can be noted that the ESR value attained at the 1st cycle was determined to be 53 Ω. Consequently, it is gradually increased with increasing cycle number until recorded its optimum value once the cycle number reaches its 100th cycle. The increment in the ESR value is resulting from an increase in the V_d value. The internal resistance in the assembled EDLC is due mainly to the utilized electrolyte for the current collector, charge–discharge method,

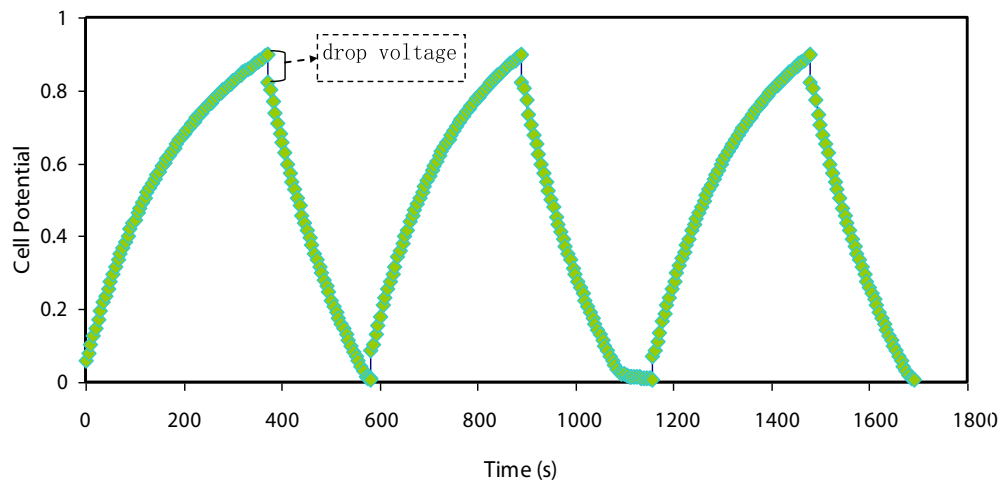


Fig. 7 The GCD curve for the manufactured EDLC cell.

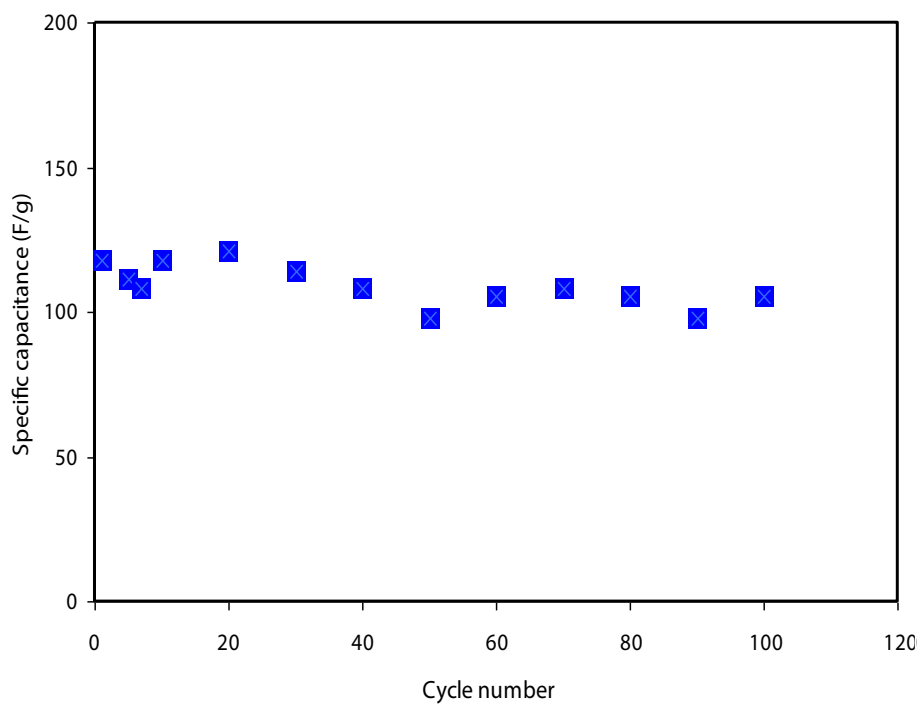


Fig. 8 The variation of specific capacitance, C_s for the constructed EDLC up to 100 cycles.

and the gap in interfacial between electrodes with polymer electrolyte (Lim et al., 2014; Gu et al., 2000; Udawatte et al., 2018).

Other crucial parameters of energy density, E_d and power density, P_d are measured using the following equations:

$$E = \frac{C_s V^2}{2} \quad (17)$$

$$P = \frac{V^2}{4m(ESR)} \quad (18)$$

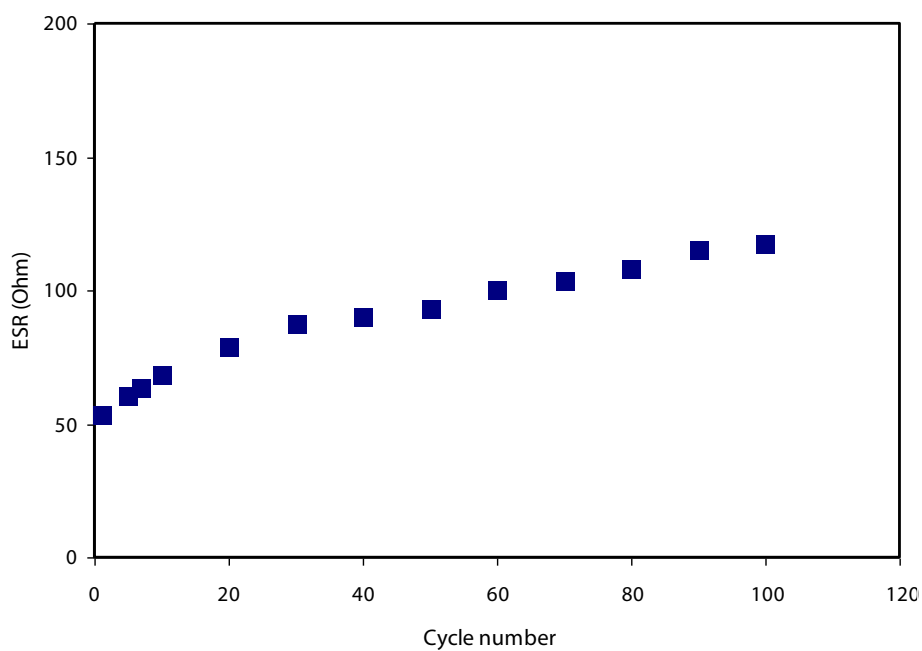


Fig. 9 The ESR value against cycle numbers up to 100 cycles.

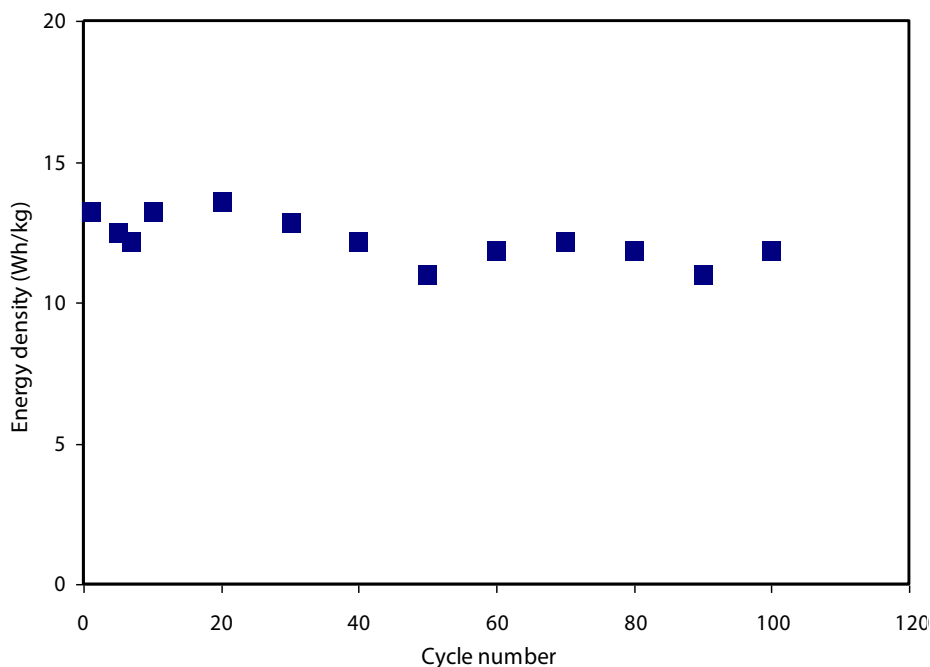


Fig. 10 Energy density (E_d) for the assembled EDLC throughout 100 cycles.

where V stands for the applied potential. Figs. 10 and 11 give information about energy density (E_d) and power density (P_d) for the assembled EDLC, respectively. According to Fig. 10, the E_d value was identified to be 13.2 Wh/kg at the 1st cycle. Beyond this, the E_d values are almost constant within an average value of ~ 12.3 Wh/kg. This exhibition suggests that from the 1st to its 100th cycle, the energy barrier for anions and

cations transference in the fabricated electrolyte is nearly the same. The E_d pattern is observed to be similar to the C_s pattern obtained in this study. The minor drop in the E_d value throughout 100 cycles is due to a rise in the ESR value. Hence, the loss of stored energy increases across its charge-discharge procedures (Jenkins and Morris, 1976; Suleman et al., 2016; Muchakayala et al., 2018). According to Hina et al. (2020),

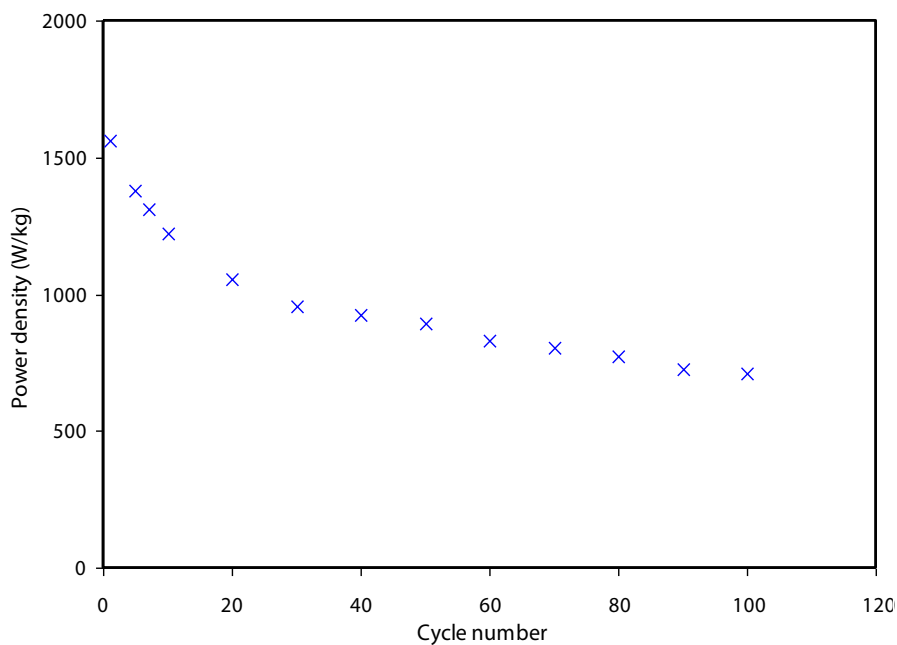


Fig. 11 Power density (P_d) for the assembled EDLC throughout 100 cycles.

the E_d value for their constructed EDLC ranged from 9.82 to 21.6 Wh/kg, depending on the content of lithium triflate (LiTf). For the carboxy methylcellulose-polyvinyl alcohol CMC-PVA system doped with ammonium bromide NH_4Br , the recorded E_d value was 1.19 Wh/kg, as reported by Mazuki et al. (2020). According to Fig. 11, the obtained value of the power density (P_d) at the 1st cycle is 1560 W/kg. Afterward, the P_d value gradually drops within a charge–discharge process. It could be linking to the depletion of the electrolyte. Ion aggregations formed following the rapid charge–discharge process, blocking ion transport to the electrode surface. As a result, ion adsorption declines at the interfaces between electrodes and electrolytes (Stepniak et al., 2016; Deng et al., 2019; Hamsan et al., 2020). The obtained initial P_d value of 757 W/kg was recorded for our previous work of glycerol system plasticized the CS-MC- NH_4I (Aziz et al., 2021). The results of energy density and power density acquired in this work are of special interest compared to other previous works as demonstrated in Table 5.

4. Conclusion

In conclusion, glycerol at three various concentrations was effectively introduced as a plasticizer into the CS-Dextran- NH_4SCN electrolyte system. The room temperature highest ionic conductivity (σ_{dc}) of (3.08×10^{-4} S/cm) has been achieved for the electrolyte incorporated with (42 wt%) of glycerol. The electrical equivalent circuits (EEC) were used to investigate the circuit elements of the electrolytes further. FTIR spectra validated the interaction and complexation between the electrolyte components. The proportion of free ions achieved from deconvolution of chosen peaks of FTIR spectra was used to calculate the transport parameters. The most ionic conductivity sample has exhibited the ions dominance with the t_{ion} of 0.95 and a decomposition voltage of 1.9 V. The value of specific capacitance (C_s) of the manufactured EDLC was determined using cyclic voltammetry (CV). The (C_s), (E_d), and (P_d) initial values were found to be 118F/g, 13.2 Wh/kg, and 1560 W/kg, respectively.

Declaration of Competing Interest

The authors declare that they have no known competing financial interests or personal relationships that could have appeared to influence the work reported in this paper.

Acknowledgments

We would like to acknowledge all support for this work by the University of Sulaimani, King Saud University, Taif University and Komar University of Science and Technology. This work was supported by Taif University Researchers Supporting Project Number (TURSP-2020/106), Taif University, Taif, Saudi Arabia. The authors (S. M. Alshehri, T. Ahmed) are grateful to the researchers supporting project number (RSP-2021/29), King Saud University, Riyadh, Saudi Arabia, for funding.

References

Arof, A.K., Amirudin, S., Yusof, S.Z., Noor, I.M., 2014. A method based on impedance spectroscopy to determine transport properties of polymer electrolytes. *Phys. Chem. Chem. Phys.* 16 (5), 1856–1867. <https://doi.org/10.1039/C3CP53830C>.

Asmara, S.N., Kufian, M.Z., Majid, S.R., Arof, A.K., 2011. Preparation and characterization of magnesium ion gel polymer electrolytes for application in electrical double layer capacitors. *Electrochim. Acta* 57, 91–97. <https://doi.org/10.1016/j.electacta.2011.06.045>.

Awasthi, P., Das, S., 2019. Reduced electrode polarization at electrode and analyte interface in impedance spectroscopy using carbon paste and paper. *Rev. Sci. Instrum.* 90 (12), 124103. <https://doi.org/10.1063/1.5123585>.

Aziz, S.B., Hamsan, M.H., Brza, M.A., Kadir, M.F.Z., Abdulwahid, R.T., Ghareeb, H.O., Woo, H.J., 2019. Fabrication of energy storage EDLC device based on CS:PEO polymer blend electrolytes with high Li^+ ion transference number. *Results Phys.* 15, 102584. <https://doi.org/10.1016/j.rinp.2019.102584>.

Aziz, S.B., Hamsan, M.H., Karim, W.O., Kadir, M.F.Z., Brza, M.A., Abdullah, O.G., 2019. High Proton Conducting Polymer Blend Electrolytes Based on Chitosan: Dextran with Constant Specific Capacitance and Energy Density. *Biomolecules* 9 (7), 267. <https://doi.org/10.3390/biom9070267>.

Aziz, S.B., Hamsan, M., Brza, M., Kadir, M., Muzakir, S., Abdulwahid, R.T., 2020. Effect of glycerol on EDLC characteristics of chitosan: Methylcellulose polymer blend electrolytes. *J. Mater. Res. Technol.* 9, 8355–8366.

Aziz, S.B., Hamsan, M.H., Nofal, M.M., Karim, W.O., Brevik, I., Brza, M.A., Abdulwahid, R.T., Al-Zangana, S., Kadir, M.F.Z., 2020. Structural, impedance and electrochemical characteristics of electrical double layer capacitor devices based on Chitosan: Dextran biopolymer blend electrolytes. *Polymers (Basel)* 12 (6), 1411. <https://doi.org/10.3390/polym12061411>.

Aziz, S.B., Brza, M.A., Dannoun, E.M.A., Hamsan, M.H., Hadi, J.M., Kadir, M.F.Z., Abdulwahid, R.T., 2020. The study of electrical and electrochemical properties of magnesium ion conducting CS: PVA based polymer blend electrolytes: Role of lattice energy of magnesium salts on EDLC performance. *Molecules* 25 (19), 4503. <https://doi.org/10.3390/molecules25194503>.

Aziz, S.B., Brza, M.A., Brevik, I., Hafiz, M.H., Asnawi, A.S.F.M., Yusof, Y.M., Abdulwahid, R.T., Kadir, M.F.Z., 2020. Blending and characteristics of electrochemical double-layer capacitor device assembled from plasticized proton ion conducting chitosan:Dextran: NH_4PF_6 polymer electrolytes. *Polymers (Basel)* 12 (9), 2103. <https://doi.org/10.3390/polym12092103>.

Aziz, S.B., Hadi, J.M., Dannoun, E.M.A., Abdulwahid, R.T., Saeed, S.R., Shahab Marf, A., Karim, W.O., Kadir, M.F.Z., 2020. The study of plasticized amorphous biopolymer blend electrolytes based on polyvinyl alcohol (PVA): Chitosan with high ion conductivity for energy storage electrical double-layer capacitors (EDLC) device application. *Polymers (Basel)* 12 (9), 1938. <https://doi.org/10.3390/polym12091938>.

Aziz, S.B., Asnawi, A.S.F.M., Kadir, M.F.Z., Alshehri, S.M., Ahamad, T., Yusof, Y.M., Hadi, J.M., 2021. Structural, electrical and electrochemical properties of glycerolized biopolymers based on chitosan (Cs): Methylcellulose (mc) for energy storage application. *Polymers (Basel)* 13 (8), 1183. <https://doi.org/10.3390/polym13081183>.

Aziz, S.B., Dannoun, E.M.A., Hamsan, M.H., Ghareeb, H.O., Nofal, M.M., Karim, W.O., Asnawi, A.S.F.M., Hadi, J.M., Kadir, M.F.Z.A., 2021. A polymer blend electrolyte based on cs with enhanced ion transport and electrochemical properties for electrical double layer capacitor applications. *Polymers (Basel)* 13, 930. <https://doi.org/10.3390/polym13060930>.

Aziz, S.B., Asnawi, A.S.F.M., Abdulwahid, R.T., Ghareeb, H.O., Alshehri, S.M., Ahamad, T., Hadi, J.M., Kadir, M.F.Z., 2021. Design of potassium ion conducting PVA based polymer electrolyte with improved ion transport properties for EDLC device application. *J. Mater. Res. Technol.* 13, 933–946. <https://doi.org/10.1016/j.jmrt.2021.05.017>.

Aziz, S.B., Nofal, M.M., Ghareeb, H.O., Dannoun, E.M.A., Hussen, S.A., Hadi, J.M., Ahmed, K.K., Hussein, A.M., 2021. Character-

- istics of poly(Vinyl alcohol) (PVA) based composites integrated with green synthesized Al_3+ -metal complex: Structural, optical, and localized density of state analysis. *Polymers (Basel)*. 13, 1–23. <https://doi.org/10.3390/polym13081316>.
- Aziz, S.B., Brza, M.A., Hamsan, H.M., Kadir, M.F.Z., Abdulwahid, R.T., 2021. Electrochemical characteristics of solid state double-layer capacitor constructed from proton conducting chitosan-based polymer blend electrolytes. *Polym. Bull.* 78 (6), 3149–3167. <https://doi.org/10.1007/s00289-020-03278-1>.
- Aziz, S.B., Nofal, M.M., Kadir, M.F.Z., Dannoun, E.M.A., Brza, M.A., Hadi, J.M., Abdulla, R.M., 2021. Bio-Based Plasticized PVA Based Polymer Blend Electrolytes and Electrochemical Properties. *Materials (Basel)*. 14, 1994.
- Brza, M.A., Aziz, S.B., Anuar, H., Ali, F., 2020. Structural, ion transport parameter and electrochemical properties of plasticized polymer composite electrolyte based on PVA: A novel approach to fabricate high performance EDLC devices. *Polym. Test.* 91, 106813. <https://doi.org/10.1016/j.polymertesting.2020.106813>.
- Brza, M., Aziz, S., Anuar, H., Alshehri, S., Ali, F., Ahamad, T., Hadi, J., 2021. Characteristics of a plasticized pva-based polymer electrolyte membrane and h+ conductor for an electrical double-layer capacitor: Structural, morphological, and ion transport properties. *Membranes (Basel)* 11 (4), 296. <https://doi.org/10.3390/membranes11040296>.
- Chai, M.N., Isa, M.I.N., 2016. Novel Proton Conducting Solid Biopolymer Electrolytes Based on Carboxymethyl Cellulose Doped with Oleic Acid and Plasticized with Glycerol. *Sci. Rep.* 6, 1–7. <https://doi.org/10.1038/srep27328>.
- Chen, W., Beidaghi, M., Penmatsa, V., Bechtold, K., Kumari, L., Li, W.Z., Wang, C., 2010. Integration of carbon nanotubes to C-MEMS for on-chip supercapacitors. *IEEE Trans. Nanotechnol.* 9, 734–740. <https://doi.org/10.1109/TNANO.2010.2049500>.
- Chong Mee Yoke, 2017. Development of biodegradable solid polymer electrolytes incorporating different nanoparticles for electric double layer capacitor (Doctoral thesis). University of Malaya, Malaysia.
- Deng, J., Li, J., Xiao, Z., Song, S., Li, L., 2019. Studies on possible ion-confinement in Nanopore for enhanced supercapacitor performance in 4V EMIBF₄ ionic liquids. *Nanomaterials (Basel)* 9 (12), 1664. <https://doi.org/10.3390/nano9121664>.
- Du, B.-W., Hu, S.-Y., Singh, R., Tsai, T.-T., Lin, C.-C., Ko, F.-H., 2017. Eco-friendly and biodegradable biopolymer chitosan/Y2O₃ composite materials in flexible organic thin-film transistors. *Materials (Basel)* 10 (9), 1026. <https://doi.org/10.3390/ma10091026>.
- Dumitrașcu, M., Meltzer, V., Sima, E., Virgolici, M.G., Albu, M.G., Ficaï, A., Moise, V., Minea, R., Vancea, C., Scărișoreanu, A., et al., 2011. characterization of electron beam irradiated collagen-polyvinylpyrrolidone (PVP) and collagen-dextran (DEX) blends. *Dig. J. Nanomater. Biostructures* 6, 1793–1803.
- Dumitrașcu, M., Albu, M.G., Virgolici, M., Vancea, C., Meltzer, V., 2012. Characterization of electron beam irradiated polyvinylpyrrolidone-dextran (PVP/DEX) blends. *Solid State Phenom.* 188, 102–108. <https://doi.org/10.4028/www.scientific.net/SSP.188.102>.
- Gu, H.-B., Kim, J.-U., Song, H.-W., Park, G.-C., Park, B.-K., 2000. Electrochemical properties of carbon composite electrode with polymer electrolyte for electric double-layer capacitor. *Electrochim. Acta* 45 (8-9), 1533–1536.
- Hadi, J.M., Aziz, S.B., Mustafa, M.S., Hamsan, M.H., Abdulwahid, R.T., Kadir, M.F.Z., Ghareeb, H.O., 2020. Role of nano-capacitor on dielectric constant enhancement in PEO:NH₄SCN:xCeO₂ polymer nano-composites: Electrical and electrochemical properties. *J. Mater. Res. Technol.* 9 (4), 9283–9294. <https://doi.org/10.1016/j.jmrt.2020.06.022>.
- Hadi, J.M., Aziz, S.B., Nofal, M.M., Hussien, S.A., Hamsan, M.H., Brza, M.A., Abdulwahid, R.T., Kadir, M.F.Z., Woo, H.J., 2020. Electrical, dielectric property and electrochemical performances of plasticized silver ion-conducting chitosan-based polymer nanocomposites. *Membranes (Basel)*. 10, 1–22. <https://doi.org/10.3390/membranes10070151>.
- Hadi, J.M., Aziz, S.B., Saeed, S.R., Brza, M.A., Abdulwahid, R.T., Hamsan, M.H., Abdullah, R.M., Kadir, M.F.Z., Muzakir, S.K., 2020. Investigation of ion transport parameters and electrochemical performance of plasticized biocompatible chitosan-based proton conducting polymer composite electrolytes. *Membranes (Basel)*. 10, 1–27. <https://doi.org/10.3390/membranes10110363>.
- Hadi, J.M., Aziz, S.B., Mustafa, M.S., Brza, M.A., Hamsan, M.H., Kadir, M.F.Z., Ghareeb, H.O., Hussein, S.A., 2020. Electrochemical impedance study of proton conducting polymer electrolytes based on PVC doped with thiocyanate and plasticized with glycerol. *Int. J. Electrochem. Sci.* 15, 4671–4683. <https://doi.org/10.20964/2020.05.34>.
- Hamsan, M.H., Shukur, M.F., Kadir, M.F.Z., 2017. NH₄NO₃ as charge carrier contributor in glycerolized potato starch-methyl cellulose blend-based polymer electrolyte and the application in electrochemical double-layer capacitor. *Ionics (Kiel)*. 23 (12), 3429–3453. <https://doi.org/10.1007/s11581-017-2155-1>.
- Hamsan, M.H., Shukur, M.F., Aziz, S.B., Kadir, M.F.Z., 2019. Dextran from *Leuconostoc mesenteroides*-doped ammonium salt-based green polymer electrolyte. *Bull. Mater. Sci.* 42. <https://doi.org/10.1007/s12034-019-1740-5>.
- Hamsan, M.H., Shukur, M.F., Aziz, S.B., Yusof, Y.M., Kadir, M.F.Z., 2020. Influence of NH₄ Br as an ionic source on the structural/electrical properties of dextran-based biopolymer electrolytes and EDLC application. *Bull. Mater. Sci.* 43. <https://doi.org/10.1007/s12034-019-2008-9>.
- Hamsan, M.H., Aziz, S.B., Nofal, M.M., Brza, M.A., Abdulwahid, R.T., Hadi, J.M., Karim, W.O., Kadir, M.F.Z., 2020. Characteristics of EDLC device fabricated from plasticized chitosan:MgCl₂ based polymer electrolyte. *J. Mater. Res. Technol.* 9 (5), 10635–10646. <https://doi.org/10.1016/j.jmrt.2020.07.096>.
- Hamsan, M.H., Aziz, S.B., Azha, M.A.S., Azli, A.A., Shukur, M.F., Yusof, Y.M., Muzakir, S.K., Manan, N.S.A., Kadir, M.F.Z., 2020. Solid-state double layer capacitors and protonic cell fabricated with dextran from *Leuconostoc mesenteroides* based green polymer electrolyte. *Mater. Chem. Phys.* 241, 122290. <https://doi.org/10.1016/j.matchemphys.2019.122290>.
- Hemalatha, R., Alagar, M., Selvasekarapandian, S., Sundaresan, B., Moniha, V., 2019. Studies of proton conducting polymer electrolyte based on PVA, amino acid proline and NH₄ SCN. *J. Sci. Adv. Mater. Devices* 4 (1), 101–110. <https://doi.org/10.1016/j.jsamd.2019.01.004>.
- Hina, M., Bashir, S., Kamran, K., Ramesh, S., Ramesh, K., 2020. Synthesis and characterization of self-healable poly (acrylamide) hydrogel electrolytes and their application in fabrication of aqueous supercapacitors. *Polymer (Guildf)*. 210, 123020. <https://doi.org/10.1016/j.polymer.2020.123020>.
- Iro, Z.S., Subramani, C., Dash, S.S., 2016. A brief review on electrode materials for supercapacitor. *Int. J. Electrochem. Sci.* 11, 10628–10643. <https://doi.org/10.20964/2016.12.50>.
- Jenkins, H.D.D.B., Morris, D.F., 1976. C, A new estimation of the lattice energies of the ammonium halides and the proton affinity of gaseous ammonia. *Molecular Physics* 32, 231–236.
- Kadir, M.F.Z., Arof, A.K., 2011. Application of PVA-chitosan blend polymer electrolyte membrane in electrical double layer capacitor. *Mater. Res. Innov.* 15 (sup2), s217–s220.
- Kadir, M.F.Z., Hamsan, M.H., 2018. Green electrolytes based on dextran-chitosan blend and the effect of NH₄SCN as proton provider on the electrical response studies. *Ionics (Kiel)*. 24 (8), 2379–2398. <https://doi.org/10.1007/s11581-017-2380-7>.
- Kiamahalleh, M.V., Zein, S.H.S., Najafpour, G., Sata, S.A., Buniran, S., 2012. Multiwalled carbon nanotubes based nanocomposites for supercapacitors: A review of electrode materials. *Nano* 07 (02), 1230002. <https://doi.org/10.1142/S1793292012300022>.
- Kumar, Y., Pandey, G.P., Hashmi, S.A., 2012. Gel polymer electrolyte based electrical double layer capacitors: Comparative study with

- multiwalled carbon nanotubes and activated carbon electrodes. *J. Phys. Chem. C* 116 (50), 26118–26127. <https://doi.org/10.1021/jp305128z>.
- Liang, S., Huang, Q., Liu, L., Yam, K.L., 2009. Microstructure and molecular interaction in glycerol plasticized chitosan/poly(vinyl alcohol) blending films. *Macromol. Chem. Phys.* 210 (10), 832–839. <https://doi.org/10.1002/macp.v210:1010.1002/macp.200900053>.
- Liew, C.-W., Ramesh, S., Arof, A.K., 2016. Enhanced capacitance of EDLCs (electrical double layer capacitors) based on ionic liquid-added polymer electrolytes. *Energy* 109, 546–556.
- Lim, C.-S., Teoh, K., Liew, C.-W., Ramesh, S., 2014. Capacitive behavior studies on electrical double layer capacitor using poly (vinyl alcohol)-lithium perchlorate based polymer electrolyte incorporated with TiO₂. *Mater. Chem. Phys.* 143, 661–667.
- Lim, C.-S., Teoh, K.H., Liew, C.-W., Ramesh, S., 2014. Electric double layer capacitor based on activated carbon electrode and biodegradable composite polymer electrolyte. *Ionics* 20 (2), 251–258.
- Luo, X., Wang, J., Dooner, M., Clarke, J., 2015. Overview of current development in electrical energy storage technologies and the application potential in power system operation. *Appl. Energy* 137, 511–536. <https://doi.org/10.1016/j.apenergy.2014.09.081>.
- Maheshwari, T., Tamilarasan, K., Selvasekarapandian, S., Chitra, R., Kiruthika, S., 2021. Investigation of blend biopolymer electrolytes based on Dextran-PVA with ammonium thiocyanate. *J. Solid State Electrochem.* 25 (3), 755–765. <https://doi.org/10.1007/s10008-020-04850-5>.
- Malathi, J., Kumaravadivel, M., Brahmanandhan, G.M., Hema, M., Baskaran, R., Selvasekarapandian, S., 2010. Structural, thermal and electrical properties of PVA-LiCF₃SO₃ polymer electrolyte. *J. Non. Cryst. Solids* 356 (43), 2277–2281. <https://doi.org/10.1016/j.jnoncrysol.2010.08.011>.
- Mazuki, N., Abdul Majeed, A.P.P., Samsudin, A.S., 2020. Study on electrochemical properties of CMC-PVA doped NH₄Br based solid polymer electrolytes system as application for EDLC. *J. Polym. Res.* 27, 135. <https://doi.org/10.1007/s10965-020-02078-5>.
- Mobarak, N.N., Ahmad, A., Abdullah, M.P., Ramli, N., Rahman, M. Y.A., 2013. Conductivity enhancement via chemical modification of chitosan based green polymer electrolyte. *Electrochim. Acta* 92, 161–167. <https://doi.org/10.1016/j.electacta.2012.12.126>.
- Mohamed, A.S., Shukur, M.F., Kadir, M.F.Z., Yusof, Y.M., 2020. Ion conduction in chitosan-starch blend based polymer electrolyte with ammonium thiocyanate as charge provider. *J. Polym. Res.* 27 (6). <https://doi.org/10.1007/s10965-020-02084-7>.
- Muchakayala, R., Song, S., Wang, J., Fan, Y., Benggeppagari, M., Chen, J., Tan, M., 2018. Development and supercapacitor application of ionic liquid-incorporated gel polymer electrolyte films. *J. Ind. Eng. Chem.* 59, 79–89. <https://doi.org/10.1016/j.jiec.2017.10.009>.
- Mustafa, M.S., Ghareeb, H.O., Aziz, S.B., Brza, M.A., Al-zangana, S., Hadi, J.M., Kadir, M.F.Z., 2020. Electrochemical characteristics of glycerolized PEO-based polymer electrolytes. *Membranes* (Basel). 10, 1–16. <https://doi.org/10.3390/membranes10060116>.
- Nadiah, N.S., Mahipal, Y.K., Numan, A., Ramesh, S., Ramesh, K., 2015. Efficiency of supercapacitor using EC/DMC-based liquid electrolytes with methyl methacrylate (MMA) monomer. *Ionics* 22, 107–114.
- Nadiah, N.S., Omar, F.S., Numan, A., Mahipal, Y.K., Ramesh, S., Ramesh, K., 2017. Influence of acrylic acid on ethylene carbonate/dimethyl carbonate based liquid electrolyte and its supercapacitor application. *Int. J. Hydrogen Energy* 42 (52), 30683–30690. <https://doi.org/10.1016/j.ijhydene.2017.10.140>.
- Nasef, M.M., Saidi, H., Dahlan, K.Z.M., 2007. Preparation of composite polymer electrolytes by electron beam-induced grafting: Proton- and lithium ion-conducting membranes. *Nucl. Instruments Methods Phys. Res. Sect. B Beam Interact. with Mater. Atoms* 265 (1), 168–172. <https://doi.org/10.1016/j.nimb.2007.08.044>.
- NG, L., MOHAMAD, A., 2008. Effect of temperature on the performance of proton batteries based on chitosan-NH₄NO₃-EC membrane. *J. Memb. Sci.* 325 (2), 653–657. <https://doi.org/10.1016/j.memsci.2008.08.029>.
- Nik Aziz, N.A., Idris, N.K., Isa, M.I.N., 2010. Solid polymer electrolytes based on methylcellulose: FT-IR and ionic conductivity studies. *Int. J. Polym. Anal. Charact.* 15 (5), 319–327. <https://doi.org/10.1080/1023666X.2010.493291>.
- Nirmala Devi, G., Chitra, S., Selvasekarapandian, S., Premalatha, M., Monisha, S., Saranya, J., 2017. Synthesis and characterization of dextrin-based polymer electrolytes for potential applications in energy storage devices. *Ionics* (Kiel). 23 (12), 3377–3388. <https://doi.org/10.1007/s11581-017-2135-5>.
- Nofal, M.M., Aziz, S.B., Hadi, J.M., Abdulwahid, R.T., Dannoun, E. M.A., Marif, A.S., Al-Zangana, S., Zafar, Q., Brza, M.A., Kadir, M.F.Z., 2020. Synthesis of porous proton ion conducting solid polymer blend electrolytes based on PVA: CS polymers: Structural, morphological and electrochemical properties. *Materials* (Basel). 13, 1–21. <https://doi.org/10.3390/ma13214890>.
- Nofal, M.M., Aziz, S.B., Hadi, J.M., Karim, W.O., Dannoun, E.M.A., Hussein, A.M., Hussien, S.A., 2021. Optical Energy Band Gap Using a Promising Green Methodology. *Structural and Optical Properties*.
- Noor, N.A.M., Isa, M.I.N., 2019. Investigation on transport and thermal studies of solid polymer electrolyte based on carboxymethyl cellulose doped ammonium thiocyanate for potential application in electrochemical devices. *International Journal of Hydrogen Energy*. 44 (16), 8298–8306.
- Pandey, G.P., Kumar, Y., Hashmi, S., 2011. Ionic liquid incorporated PEO based polymer electrolyte for electrical double layer capacitors: A comparative study with lithium and magnesium systems. *Solid State Ion.* 190, 93–98.
- Polu, A.R., Kumar, R., 2011. AC impedance and dielectric spectroscopic studies of Mg²⁺ ion conducting PVA-PEG blended polymer electrolytes. *Bull. Mater. Sci.* 34, 1063–1067. <https://doi.org/10.1007/s12034-011-0132-2>.
- Polu, A.R., Kumar, R., 2013. Ionic conductivity and discharge characteristic studies of PVA-Mg(CH₃COO)₂ solid polymer electrolytes. *Int. J. Polym. Mater. Polym. Biomater.* 62 (2), 76–80. <https://doi.org/10.1080/00914037.2012.664211>.
- Qian, X., Gu, N., Cheng, Z., Yang, X., Wang, E., Dong, S., 2001. Impedance study of (PEO)₁₀LiClO₄-Al₂O₃ composite polymer electrolyte with blocking electrodes. *Electrochim. Acta* 46 (12), 1829–1836. [https://doi.org/10.1016/S0013-4686\(00\)00723-4](https://doi.org/10.1016/S0013-4686(00)00723-4).
- Ramlli, M.A., Isa, M.I.N., 2016. Structural and ionic transport properties of protonic conducting solid biopolymer electrolytes based on carboxymethyl cellulose doped with ammonium fluoride. *J. Phys. Chem. B* 120 (44), 11567–11573. <https://doi.org/10.1021/acs.jpcc.6b06068>.
- Ramya, C.S., Selvasekarapandian, S., Savitha, T., Hirankumar, G., Angelo, P.C., 2007. Vibrational and impedance spectroscopic study on PVP-NH₄SCN based polymer electrolytes. *Physica B* 393 (1-2), 11–17.
- Rani, M.S.A., Dzulkurnain, N.A., Ahmad, A., Mohamed, N.S., 2015. Conductivity and Dielectric Behavior Studies of Carboxymethyl Cellulose from Kenaf Bast Fiber Incorporated with Ammonium Acetate-BMATFSI Biopolymer Electrolytes. *Int. J. Polym. Anal. Charact.* 20 (3), 250–260. <https://doi.org/10.1080/1023666X.2015.1013176>.
- Rani, M.S.A., Ahmad, A., Mohamed, N.S., 2018. Influence of nano-sized fumed silica on physicochemical and electrochemical properties of cellulose derivatives-ionic liquid biopolymer electrolytes. *Ionics* (Kiel). 24 (3), 807–814. <https://doi.org/10.1007/s11581-017-2235-2>.
- Sampathkumar, L., Christopher Selvin, P., Selvasekarapandian, S., Perumal, P., Chitra, R., Muthukrishnan, M., 2019. Synthesis and characterization of biopolymer electrolyte based on tamarind seed polysaccharide, lithium perchlorate and ethylene carbonate for electrochemical applications. *Ionics* (Kiel). 25 (3), 1067–1082. <https://doi.org/10.1007/s11581-019-02857-1>.

- Samsudin, A.S., Isa, M.I.N., 2012. Characterization of carboxy methylcellulose doped with DTAB as new types of biopolymer electrolytes. *Bull. Mater. Sci.* 35 (7), 1123–1131. <https://doi.org/10.1007/s12034-012-0396-1>.
- Samsudin, A.S., Lai, H.M., Isa, M.I.N., 2014. Biopolymer materials based carboxymethyl cellulose as a proton conducting biopolymer electrolyte for application in rechargeable proton battery. *Electrochim. Acta* 129, 1–13. <https://doi.org/10.1016/j.electacta.2014.02.074>.
- Selvalakshmi, S., Vijaya, N., Selvasekarapandian, S., Premalatha, M., 2017. Biopolymer agar-agar doped with NH₄SCN as solid polymer electrolyte for electrochemical cell application. *J. Appl. Polym. Sci.* 134, 1–10. <https://doi.org/10.1002/app.44702>.
- Shamsuri, N.A., Zaine, S.N.A., Yusof, Y.M., Yahya, W.Z.N., Shukur, M.F., 2020. Effect of ammonium thiocyanate on ionic conductivity and thermal properties of polyvinyl alcohol–methylcellulose–based polymer electrolytes. *Ionics (Kiel)*. 26 (12), 6083–6093. <https://doi.org/10.1007/s11581-020-03753-9>.
- Shanmuga Priya, S., Karthika, M., Selvasekarapandian, S., Manjuladevi, R., 2018. Preparation and characterization of polymer electrolyte based on biopolymer I-Carrageenan with magnesium nitrate. *Solid State Ionics* 327, 136–149. <https://doi.org/10.1016/j.ssi.2018.10.031>.
- Shobana, V., Parthiban, P., Balakrishnan, K., 2015. Review Article Lithium based battery-type cathode material for hybrid supercapacitor, vol. 7, pp. 207–212.
- Shuhaimi, N.E.A., Teo, L.P., Woo, H.J., Majid, S.R., Arof, A.K., 2012. Electrical double-layer capacitors with plasticized polymer electrolyte based on methyl cellulose. *Polym. Bull.* 69 (7), 807–826. <https://doi.org/10.1007/s00289-012-0763-5>.
- Shukur, M.F., Ithnin, R., Kadir, M.F.Z., 2016. Ionic conductivity and dielectric properties of potato starch-magnesium acetate biopolymer electrolytes: the effect of glycerol and 1-butyl-3-methylimidazolium chloride. *Ionics (Kiel)*. 22 (7), 1113–1123. <https://doi.org/10.1007/s11581-015-1627-4>.
- Shukur, M.F., Hamsan, M.H., Kadir, M.F.Z., 2019. Investigation of plasticized ionic conductor based on chitosan and ammonium bromide for EDLC application. *Mater. Today Proc.* 17, 490–498. <https://doi.org/10.1016/j.matpr.2019.06.490>.
- Stepniak, I., Galinski, M., Nowacki, K., Wysokowski, M., Jakubowska, P., Bazhenov, V.V., Leisegang, T., Ehrlich, H., Jesionowski, T., 2016. A novel chitosan/sponge chitin origin material as a membrane for supercapacitors – preparation and characterization. *RSC Adv* 6 (5), 4007–4013.
- Suleman, M., Deraman, M., Othman, M.A.R., Omar, R., Hashim, M. A., Basri, N.H., Nor, N.S.M., Dolah, B.N.M., Hanappi, M.F.Y. M., Hamdan, E., Sazali, N.E.S., Tajuddin, N.S.M., Jasni, M.R.M., 2016. Electric double-layer capacitors with tea waste derived activated carbon electrodes and plastic crystal based flexible gel polymer electrolytes. *J. Phys. Conf. Ser.* 739, 012086. <https://doi.org/10.1088/1742-6596/739/1/012086>.
- Udawatte, G.K., Perera, K.S., Vidanapathirana, K.P., 2018. A gel polymer electrolyte based on PVdF and ZnCl₂ for an electrochemical double layer capacitor. *Ceylon J. Sci.* 47, 331–336.
- Vettori, M.H.P.B., Franchetti, S.M.M., Contiero, J., 2012. Structural characterization of a new dextran with a low degree of branching produced by *Leuconostoc mesenteroides* FT045B dextranucrase. *Carbohydr. Polym.* 88 (4), 1440–1444. <https://doi.org/10.1016/j.carbpol.2012.02.048>.
- Wang, J., Zhao, Z., Song, S., Ma, Q., Liu, R., 2018. High performance poly(vinyl alcohol)-based Li-ion conducting gel polymer electrolyte films for electric double-layer capacitors. *Polymers (Basel)*. 10, 1179. <https://doi.org/10.3390/polym10111179>.
- Wang, J., Zhao, Z., Song, S., Ma, Q., Liu, R., 2018. Zejia Zhao, Shenhua Song, Qing Ma and Renchen Liu (2018) High Performance Poly(vinyl alcohol)-Based Li-Ion Conducting Gel Polymer Electrolyte Films for Electric Double-Layer Capacitors. *Polymers* 10 (11), 1179. <https://doi.org/10.3390/polym10111179>.
- Wei, D., Sun, W., Qian, W., Ye, Y., Ma, X., 2009. The synthesis of chitosan-based silver nanoparticles and their antibacterial activity. *Carbohydr. Res.* 344 (17), 2375–2382. <https://doi.org/10.1016/j.carres.2009.09.001>.
- Woo, H.J., Majid, S.R., Arof, A.K., 2011. Conduction and thermal properties of a proton conducting polymer electrolyte based on poly (ϵ -caprolactone). *Solid State Ionics* 199–200, 14–20. <https://doi.org/10.1016/j.ssi.2011.07.007>.
- Zhang, H., Xuan, X., Wang, J., Wang, H., 2003. FT-IR investigations of ion association in PEO-MSCN (M=Na, K) polymer electrolytes. *Solid State Ionics* 164, 73–79.
- Zhu, Y.S., Xiao, S.Y., Li, M.X., Chang, Z., Wang, F.X., Gao, J., Wu, Y.P., 2015. Natural macromolecule based carboxymethyl cellulose as a gel polymer electrolyte with adjustable porosity for lithium ion batteries. *J. Power Sources* 288, 368–375. <https://doi.org/10.1016/j.jpowsour.2015.04.117>.